Journal of Organometallic Chemistry 694 (2009) 868–873

Contents lists available at ScienceDirect

Journal of Organometallic Chemistry

journal homepage: www.elsevier.com/locate/jorganchem

DFT investigation of the interaction between gold(I) complexes and the active site of thioredoxin reductase

James A.S. Howell *

School of Physical and Geographical Sciences, Lennard-Jones Laboratory, Keele University, Keele, Staffordshire ST5 5BG, United Kingdom

ARTICLE INFO

Article history:
Received 22 August 2008
Received in revised form 7 October 2008
Accepted 8 October 2008
Available online 22 October 2008

Dedicated to Professor Gerard Jaouen on the occasion of his 65th birthday

Keywords:
DFT
Gold
Thioredoxin reductase
Anticancer

ABSTRACT

The binding of the $[Au(PMe_3)]^+$ fragment to cysteine, selenocysteine and the tetrapeptides H_2NGlyCysA-GlyCOOH (A = Cys, Sec) has been investigated by DFT methods as a model for the binding of gold(I) to the selenium-containing active site of thioredoxin reductase. The calculations demonstrate both a higher acidity of Se–H compared to S–H and a stronger binding of gold at the selenium site compared to sulphur. Se–H dissociation at the selenium site increases the reducing power of the tetrapeptide H_2NGlyCysSec-GlyCOOH whilst gold coordination at selenium has the opposite effect.

1. Introduction

The chemistry of gold has recently undergone a renaissance due to new or renewed interest in areas as diverse as optical properties [1a–d], homogeneous and heterogeneous catalysis [2a–c] and chemotherapy [3a,b]. Following the report of anti-inflammatory properties in 1935 [4], several gold compounds have been developed for the clinical treatment of rheumatoid arthritis, namely mono- and disodium (1,2-dicarboxyethylthio)gold [mono- and disodium aurothiomalate, Myochrysine®], (3,4,5-trihydroxy-6-(hydroxymethyl)tetrahydro-2*H*-pyran-2-ylthio)gold [aurothioglucose, Solganol®] and (triethylphosphine)(3,4,5-triacetoxy-6-(acetoxymethyl)tetrahydro-2*H*-pyran-2-ylthio)gold [auranofin, Ridaura®]. Lately, gold(I)–phosphine compounds, including auranofin, have also been shown to possess anti-cancer properties and though this discovery is more recent, an understanding of the mechanism of action seems more complete [5].

The solid state structure of a human thioredoxin reductase (TRR) is shown in Fig. 1 [6]. As a class, such molecules catalyse the NADPH-dependent reduction of thioredoxins (TR). After binding of NADPH, electrons are transported *via* FAD to the N-terminal active site disulfide of one subunit and from there to the flexible C-terminal redox centre of the other subunit. This subunit is flexible and solvent exposed and contains a terminal –GlyCysSecGlyCOOH fragment which is essential for catalysis (Sec = selenocysteine [7a–c]). Mutational studies in which Sec was replaced by Cys show a marked decrease in the rate of TR reduction [8]. In terms of cytotoxicity, it has recently been proposed [9a–e] that binding of Au(I) at this active site in mitochondrial TRR promotes apoptosis since H_2O_2 produced by the mitochondrial respiratory chain oxidises reducing agents such as TR which then cannot be reduced by Au(I)-inhibited TRR. Oxidised TRR can act on several different membrane targets leading to increased permeability of the mitochondrial membranes, release of cytochrome c and eventually cell death. Specific targeting to tumour cells may depend on the elevated mitochondrial membrane potential of cancer cells.

The objective of this work is to examine by DFT methods the structure and selectivity of gold(I) complexation at this active site using a realistic model of auranofin.

2. Computational methods

DFT calculations were performed with the GAUSSIAN-03 package [10] using a LanL2DZ basis set and the B3PW91 functional. This combination has been shown to provide satisfactory results for thiolate and phosphine complexes of the coinage metals [11a,b]. Errors in geometry and bond dissociation energies are typically about 3% and 10%, respectively. Sample calculations indicated that basis set superposition errors were negligible. A complete table of minimised structures and energies can be obtained from the author.

Structures of all ground state molecules were optimised firstly in the gas phase; frequency calculations showed no imaginary

* Tel./fax: +44 1782 583041.
E-mail address: j.a.s.howell@keele.ac.uk

0022-328X/$ - see front matter © 2008 Elsevier B.V. All rights reserved.
doi:10.1016/j.jorganchem.2008.10.029

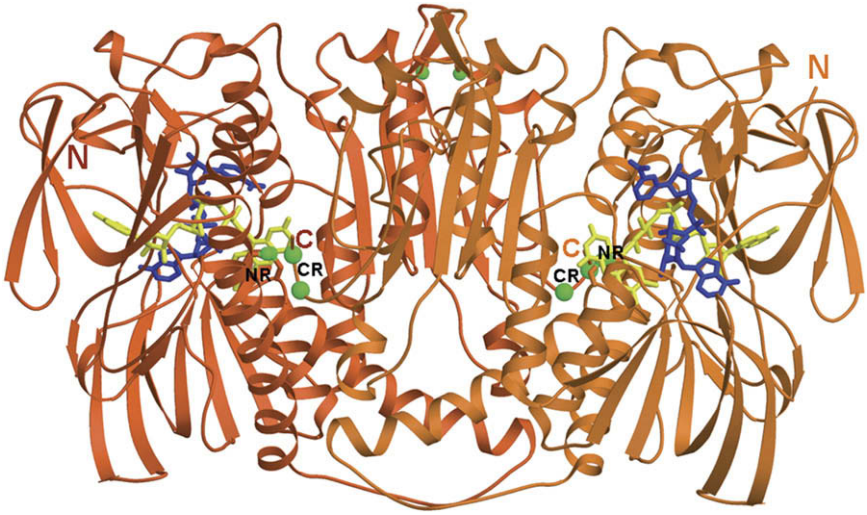

Fig. 1. Assembly of the thioredoxin reductase homodimer (reprinted with permission from Ref. [6]) The 2-fold crystallographic axis is located between the two monomers (orange and dark orange) and points almost vertically into the drawing plane. The FAD (yellow) and NADP+ (blue) molecules are shown in ball-and-stick presentation. The N-terminal and C-terminal redox centres are labelled NR and CR, respectively; N and C termini are labelled N and C respectively. The sulphur atoms of C458 and 458′, C58/63 and C58′/63′, and C497/U498 and C497/U498 are marked by green balls. (For interpretation of the references to colour in this figure legend, the reader is referred to the web version of this article.)

frequencies. Optimised aquated structures were then obtained by use of the COSMOS/RS polarised continuum model. Whilst this procedure yields ΔG^{o}_{aq} values which bear relative comparison, absolute values are not accurate. For a reaction in aqueous solution, $A_{(aq)} + B_{(aq)} \rightarrow C_{(aq)} + D_{(aq)}$, simple application of Hess's Law yields $\Delta G^{o}_{aq} = \Delta G^{o}_{gas} + \Delta G^{o}_{hyd}$ where $\Delta G^{o}_{hyd} = \Sigma G^{o}_{hyd}$ of products $- \Sigma G^{o}_{hyd}$ of reactants [12]. Both ΔG^{o}_{gas} and the hydration energies of individual chemical species can be obtained by calculation, and hence so can a value of ΔG^{0}_{aq}. However, calculated values of ΔG^{0}_{aq} ignore the solvent reorganisation induced by the solute (E_{reorg}). This term can be estimated computationally by the equation $E_{reorg} = T(\alpha/\beta)V_s$ where α and β are the coefficients of isobaric thermal expansion and isothermal compressibility of the solvent, respectively, and V_s is the partial molar volume of the solute [13]. Even with correction for solvent reorganisation, the calculated ΔG^{0}_{aq} of cysteine (-225 kJ mol^{-1}) [14] is more negative than the observed experimental value of 11.1 kJ mol^{-1} [17](something which is common to other comparisons where data is available). However, the calculated difference in pK_a for X–H ionisation (X = S, Se) of cysteine and selenocysteine (3.16) is very close to the experimental difference in pK_a for the X–H ionisation of proteins containing cysteine or selenocysteine thiol or selenol groups (~3.2) [8].

3. Results and discussion

The molecule (trimethylphosphine)(3,4,5-trihydroxy-6-(hydroxymethyl)tetrahydro-2*H*-pyran-2-ylthio)gold **1** (Fig. 2) has been used as a model for auranofin, thus replacing PEt_3 with PMe_3 and removing the acetyl protecting groups for computational simplicity. In the solid state, auranofin exhibits a monomeric molecular structure [18].

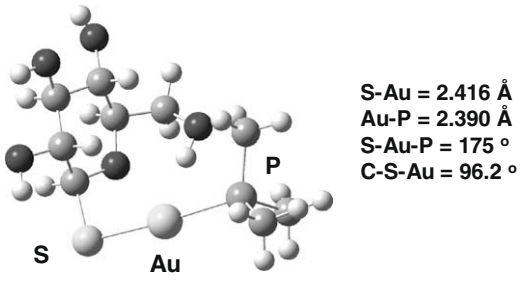

Fig. 2. Minimised structure of **1**.

Fig. 3 shows the variation in calculated p*K* for the thiolate exchange reaction (A):

$$(\text{thioglucosate})\text{Au}(\text{PMe3}) + \text{XH} \rightarrow \text{XAuL} + \text{thioglucose} \qquad \text{(A)}$$

	XH[a]	X^{-}[b]	L
2	Cys	–	–
3	Sec	–	–
4	NH_2GlyCysCysGlyCOOH	–	–
5	NH_2GlyCysSecGlyCOOH	–	–
6	–	[Cys]$^{-}$	–
7	–	[Sec]$^{-}$	–
8	–	[NH_2GlyCysCysGlyCOOH]$^{-}$	–
9	–	[NH_2GlyCysSecGlyCOOH]$^{-}$	–
10	–	[Cys]$^{-}$	PMe_3
11	–	[Sec]$^{-}$	PMe_3
12	–	[NH_2GlyCysCysGlyCOOH]$^{-}$	PMe_3
13	–	[NH_2GlyCysSecGlyCOOH]$^{-}$	PMe_3

[a]Cys = cysteine, Sec = selenocysteine, Gly = glycine.
[b]For 8, 9 and 10–13, the S/Se α to the C-terminal GlyCOOH is assumed to be the ionised site.

The following conclusions, which are based on thermodynamic preferences, assume that the activation barriers for thiol exchange are sufficiently small to rapidly provide equilibrium species distributions at approximately 298 K. It has been shown by NMR line shape analysis that the activation energies for thiol exchange between aquated (thiomalate)Au and *N*-acetylcysteine and mercaptoacetic acid are in the range 21–23 kJ mol^{-1}, with strongly negative entropies of activation indicating an associative mechanism. The rate of exchange increases with increasing pH and with increasing acidity of the S–H proton [19]. The exchange free energies in Fig. 3 are either weakly exoenergetic or weakly endoenergetic; those with p$K > 0$ are sufficiently weakly endoenergetic for the equilibrium constant to be made >1 by adjustment of the concentration of (thioglucosate)Au(PMe_3). For both pairs **2/3** and **4/5**, there is a selectivity ($\Delta pK \approx 3$–4) for complexation of the selenium site by **1**.

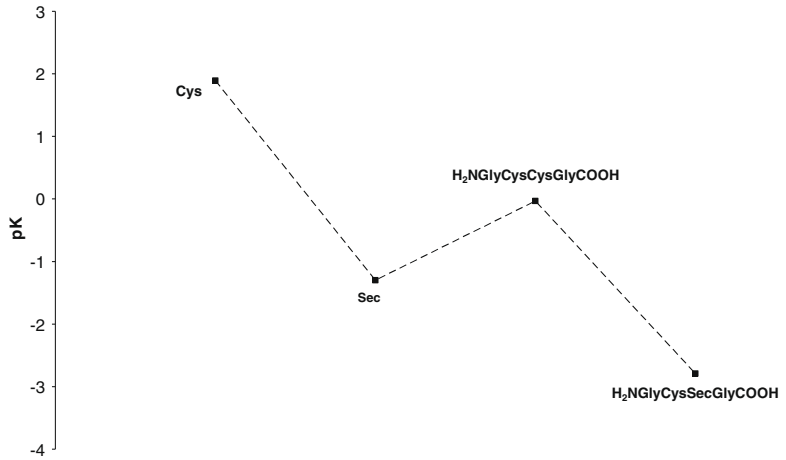

Fig. 3. Calculated p*K* values for the thiol exchange reactions of **1**.

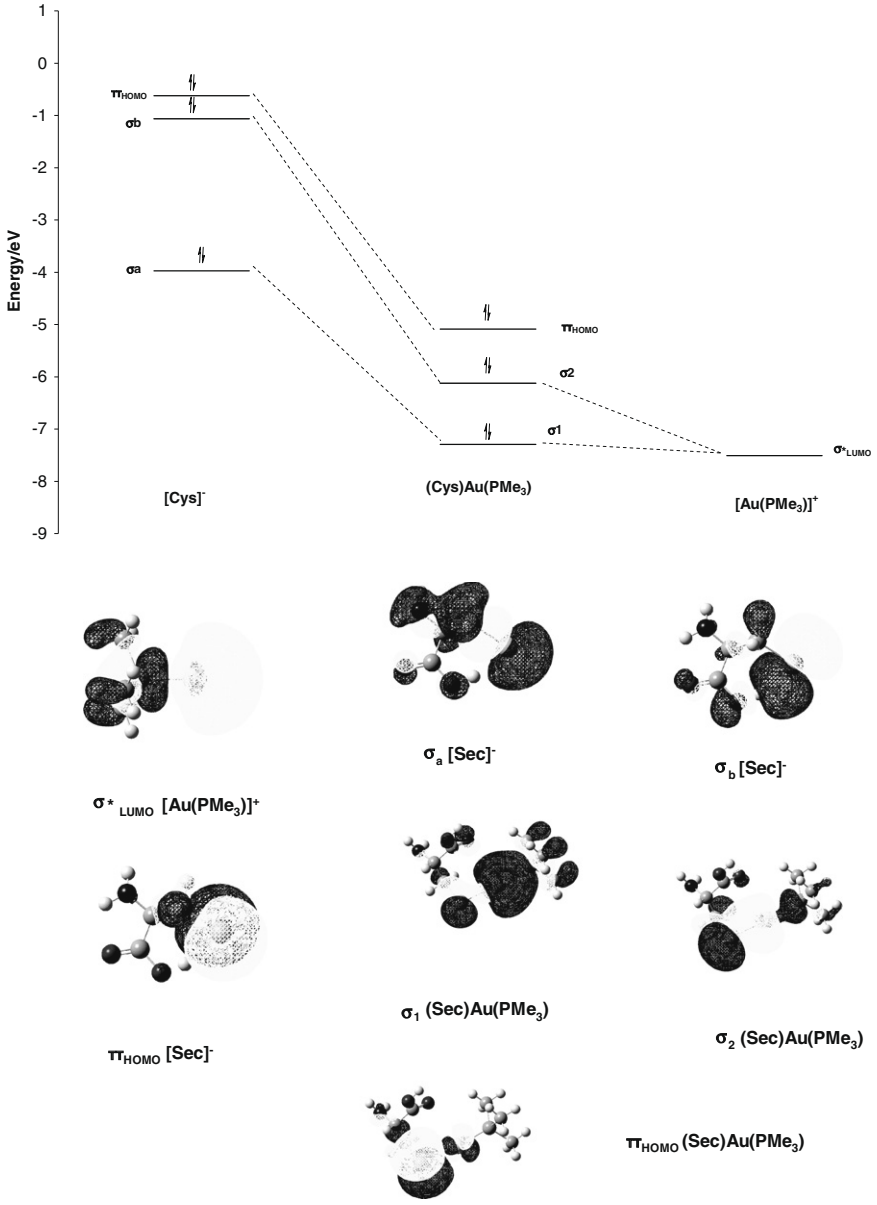

Fig. 4. Molecular orbital diagram for (Cys)Au(PMe_3)) and the shape of molecular orbitals of (Sec)Au(PMe_3).

Fig. 4 shows a molecular orbital diagram which illustrates the bonding in (Cys)Au(PMe_3) generated from the valence orbitals of $[Cys]^-$ and $[Au(PMe_3)]^+$. The acceptor orbital is the LUMO of the $[Au(PMe_3)]^+$ fragment. The valence orbitals of $[Cys]^-$ consist of two approximately orthogonal sulphur-localised lone pairs (σ_b, π_{HOMO}) together with σ_a which is primarily localised in the C–S bond. In (Cys)Au(PMe_3), the π_{HOMO} orbital remains essentially non-bonding, whereas overlap of the σ donor and acceptor orbitals generates three molecular orbitals σ_1 to σ_3, of which σ_1 and σ_2 are filled. Au(I) and thiolate are classed as a soft acid and soft base, respectively, [20]. The energies of the valence thiolate orbitals are more closely matched by the $[Au(PMe_3)]^+$ than, for example, a hard-acid containing fragment such as $[Au(H_2O)]^+$. The residual charge on the gold atom is more positive for $[Au(H_2O)]^+$ (+0.79) than for $[Au(PMe_3)]^+$ (+0.25).

Fig. 5 shows the variation in calculated pK for the acid-base reactions (B) and (C):

$$XH + H_2O \rightarrow X^- + H_3O^+, \qquad (B)$$

$$XH + [Au(H_2O)(PMe_3)]^+ \rightarrow XAu(PMe_3) + H. \qquad (C)$$

The Brønsted acidities of cysteine **2** and selenocysteine **3** are significantly enhanced compared to the tetrapeptides **4** and **5** ($\Delta pK \approx 1.5$–2) since the most stable configurations of the $[Cys]^-$ and $[Sec]^-$ monoanion are stabilised by intramolecular hydrogen bonding. Removal of either the O–H or X–H proton (X = S, Se) from the neutral amino acid results in optimisation and convergence to the analogous structures **6** and **7** (Fig. 6).

The pK values increase dramatically when the neutral amino acid is combined with the more electrophilic $[Au(H_2O)(PMe_3)]^+$ cation ($\Delta pK \approx 19$–27). The stronger X–H acidity (X = S, Se) of H_2NGlyCysSecGlyCOOH compared to H_2NGlyCysCysGlyCOOH ($\Delta pK = 1.7$) is not dissimilar to the difference in pK_{a1} between H_2S and H_2Se ($\Delta pK_a = 3.0$) [21]. As Au(I) is a soft acid, stronger complexation of selenium is consistent with the trend towards softer base character found on descending a group. Calculated C–X and Au–X distances (X = S, Se) are approximately 6% and 4% longer respectively for selenium compared to sulphur.

The much higher activity of the enzyme containing fragment **5** rather than **4** may be kinetic in origin and may also rely on the higher acidity of Se–H compared to S–H. It has been proposed [8] that the initial step in the reduction of oxidised TR may involve initial nucleophilic attack of an anion containing fragment **8** or **9** at the S–S bridge of oxidised TR. As Se–H (but not S–H) is fully ionised at biological pH, the reaction rate is enhanced. It has been recently demonstrated experimentally and by DFT calculation that selenol (Sec498) ionisation is enhanced by proton transfer to a neighbouring His472Glu477pair [22a,b]. An examination of the thermodynamic consequences for the oxidation half cells **D**, **E** and **F** has been undertaken using a value for the free energy of the aquated electron of -145 kJ mol^{-1} [23]. The oxidation potentials of these half cells represent the function of neutral **4** (taken as a reference point), ionised **9** and the complexes **12** and **13** as reducing agents. The calculated variation in oxidation potential between reactions D and E is reasonably close to that recently measured experimentally [24]. Note that Au(I)-thioether complexes are well known, and the optimised structures of **14** and **15**, the products of reaction **F**, are shown in Fig. 6.

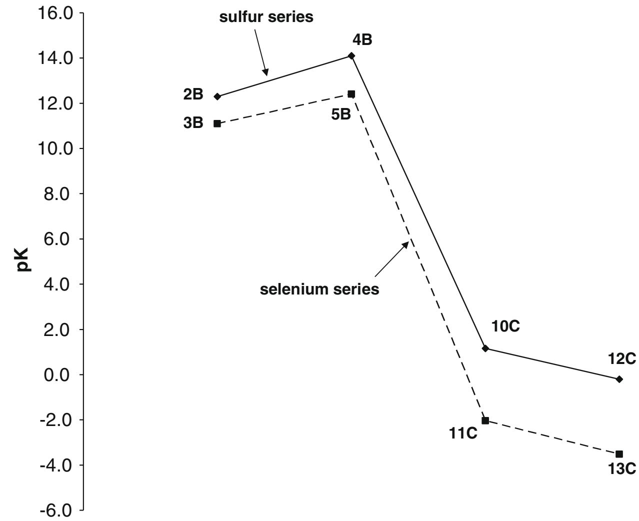

Fig. 5. Calculated pK values for the acid–base reactions **2B–5B** and **10C–13C**.

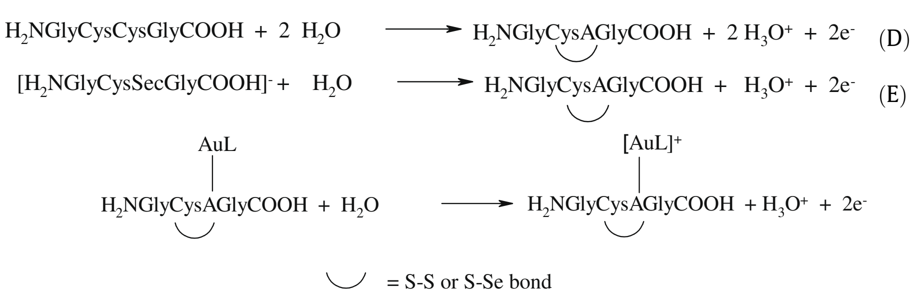

(F)

Reaction	ΔpK[a]	ΔE/mV[a]
D (A = S)	0	0
E (A = Se)	-18.1	540 (350)[b]
F (A = S)	8.0	-240
F (A = Se)	2.6	-76

[a] values relative to reaction **D**
[b] experimental value from reference 24

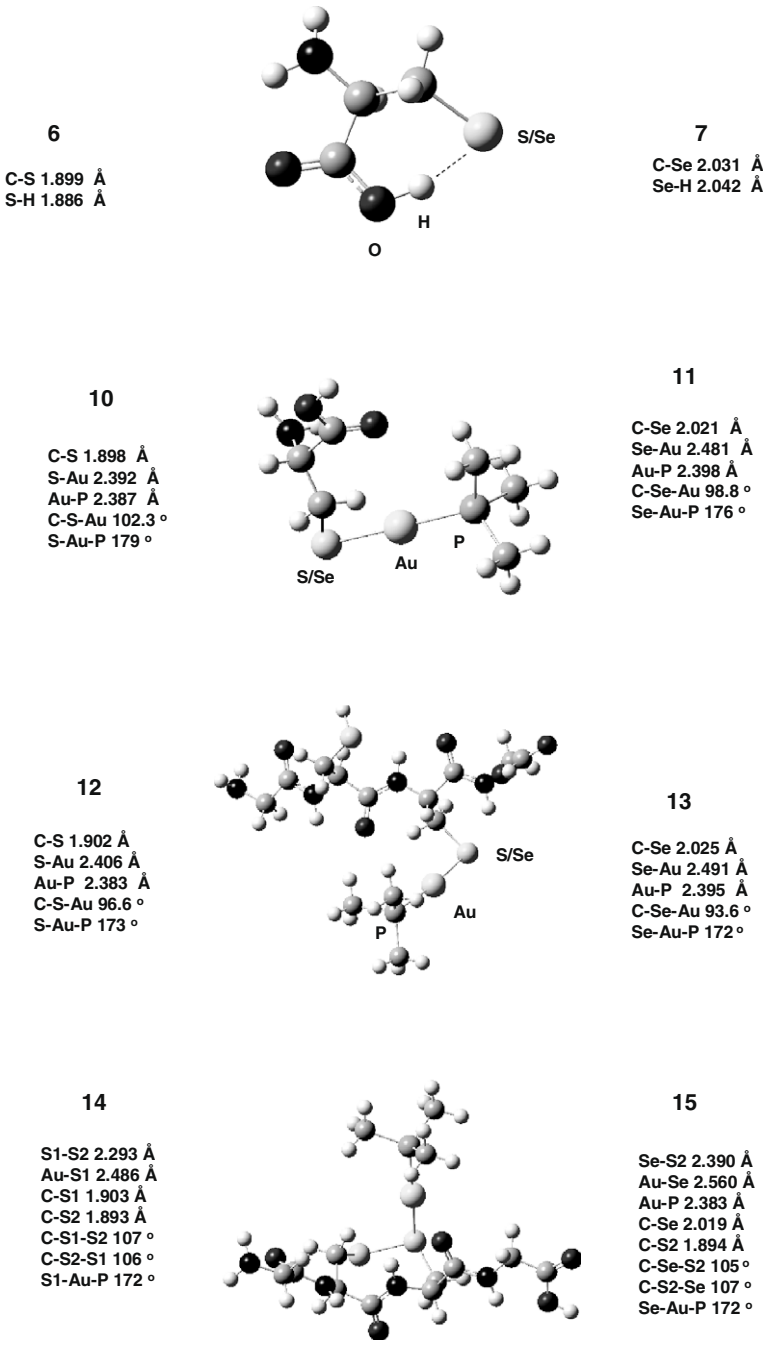

Fig. 6. Optimised structures of **6**, **7**, **10–13** and **14, 15**.

The results clearly indicate that ionisation increases the reducing power of the half cell whilst gold coordination has the opposite effect.

4. Conclusions

The binding of gold(I) as $Au(PMe_3)]^+$ to Cys, Sec and the tetrapeptides H_2NGlyCysCysGlyCOOH and H_2NGlyCysSecGlyCOOH as models for the interaction of gold(I) with the active site of thioredoxin reductase has been examined by DFT methods. The calculations are consistent with the greater activity of the selenium-containing enzyme compared to sulphur and with the mechanism proposed for the anti-cancer activity of these gold complexes.

References

[1] (a) For recent reviews, see: V.W.W. Yam, K.M.C. Wong, Top. Curr. Chem. 257 (2005) 1;
(b) E.J. Fernandez, A. Laguna, M.W. Olmos, Adv. Organomet. Chem. 52 (2005) 77;
(c) C.E. Powell, M.G. Humphrey, Coord. Chem. Rev. 248 (2004) 725;
(d) T. Goodson, O. Varnavski, Y. Yang, Int. Rev. Phys. Chem. 23 (2004) 109.
[2] (a) For recent reviews, see: A. Arcadi, Curr. Org. Chem. 8 (2004) 795;
(b) J.C. Fierro-Gonzalez, S. Kuba, Y.L. Hao, B.C. Gates, J. Phys. Chem. B 110 (2006) 13326;
(c) L. Armelao, D. Barreca, G. Bottaro, A. Gasparotto, S. Gross, C. Maragno, E. Tondello, Coord. Chem. Rev. 250 (2006) 1294.
[3] For recent reviews, see (a) E.R. Tiekink, Inflammopharmacology 16 (2008) 138;
(b) V. Milacic, D. Fregona, Q.P. Dou, Histology and Histopathology 23 (2008) 101.
[4] J. Forestier, J. Lab. Clin. Med. 20 (1935) 827.
[5] P.J. Barnard, S.J. Berners-Lee, Coord. Chem. Rev. 251 (2007) 1889.

[6] K. Fritz-Wolf, S. Urig, K. Becker, J. Mol. Biol. 370 (2007) 116.
[7] (a) T.C. Stadtman, Adv. Enzymol. Relat. Areas Mol. Biol. 48 (2006) 1;
(b) A. Wessjohann, A. Schneider, M. Abbas, W. Brandt, Biol. Chem. 388 (2007) 997;
(c) A. Bock, K. Forchhammer, J. Heider, W. Leinfelder, G. Sawers, B. Veprek, F. Zinoni, Mol. Microbiol. 5 (2006) 515.
[8] L. Gromer, H. Lohansson, J.D. Bauer, S. Arscott, D.P. Rauch, C.H. Ballour, R.H. Williams, S.J. Schirmer, E.S.J. Arner, Proc. Natl. Acad. Sci. 100 (2003) 12618. and references therein.
[9] (a) M.P. Rigobello, A. Folda, B. Dani, R. Menabo, G. Scutari, A. Bindoli, Eur. J. Pharmacol. 582 (2008) 26;
(b) C. Marzano, V. Gandin, A. Folda, G. Scutari, A. Bindoli, M.P. Rigobello, Free Rad. Biol. Med. 42 (2007) 872;
(c) M.P. Rigobello, A. Folda, M.C. Baldoin, G. Scutari, A. Bindoli, Free Rad. Res. 39 (2005) 687;
(d) M.P. Rigobello, L. Messori, G. Marcon, M.A. Cinellu, M. Bragadin, A. Folda, G. Scutari, A. Bindoli, J. Inorg. Biochem. 98 (2004) 1634;
(e) M.P. Rigobello, G. Scutari, A. Folda, A. Bindoli, Biochem. Pharmacol. 67 (2004) 689.
[10] M.J. Frisch, G.W. Trucks, H.B. Schlegel, G. E Scuseria, M.A. Robb, J.R. Cheeseman, J.A. Montgomery Jr., T. Vreven, K.N. Kudin, J.C. Burant, J.M. Millam, S.S. Ivengar, J. Tomasi, V. Barone, B. Mennucci, M. Cossi, G. Scalmani, N. Rega, G.A. Petersson, H. Nakatsuji, M. Hada, N. Ehara, K. Toyota, R. Fukuda, J. Hasegawa, M. Ishida, T. Nakajima, Y. Honda, O. Kitao, H. Nakai, M. Klene, X. Li, J.E. Knox, H.P. Hratchian, J.B. Cross, C. Adamo, J. Jaramillo, R. Gomperts, R.E. Stratmann, O. Yazyev, A.J. Austin, R. Cammi, C. Pomelli, J.W. Ochterski, P.Y. Ayala, K. Morokuma, G.A. Voth, P. Salvador, J.J. Dannenberg, V.G. Zakrzewski, S. Dapprich, A.D. Daniels, M.C. Strain, O. Farkas, D.K. Malick, A.D. Rabuck, K. Raghavachari, J.B. Foresman, J.V. Ortiz, Q. Cui, A.G. Baboul, S. Clifford, J. Cioslowski, B.B. Stefanov, G. Liu, A. Liashenko, P. Piskorz, I. Komaromi, R.L. Martin, D.J. Fox, T. Keith, M.A. Al-Laham, C.Y. Peng, A. Nanayakkara, M. Challacombe, P.M.W. Gill, B. Johnson, W. Chen, M.W. Wong, C. Gonzalez, J.A. Pople, Gaussian 03 Revision B.01, Gaussian Inc., Pittsburgh, PA, 2003.
[11] (a) G.M.S. Tong, A.C.S. Cheung, J. Phys. Chem. A 106 (2002) 11637;
(b) J.A.S. Howell, Polyhedron 25 (2006) 2993.
[12] G.P. Ford, B. Wang, J. Mol. Struct. (THEOCHEM) 490 (1999) 21.
[13] A.M. Zaichkov, M.A. Krest'yaninov, Russ. J. Gen. Chem. 78 (2008) 543.
[14] For water at 298 K, $T(\alpha/\beta) = 0.169$ kJ cm^{-3} [15] and V_s (cysteine) = 73.3 cm^3 mol^{-1} [16].
[15] D. Ben-Amotz, F.O. Rainer, G. Stell, J. Phys. Chem. B 109 (2005) 6866.
[16] F. Shahidi, P.G. Farrell, J. Chem. Soc. Farad. Trans. 1 (77) (1981) 963.
[17] B. Palecz, Amino Acids 27 (2004) 299.
[18] D.T. Hill, B.M. Sutton, Cryst. Struct. Comm. 9 (1980) 679.
[19] A.A. Isab, P.J. Sadler, J.C.S. Dalton, 1982, p. 135 and references therein.
[20] C.E. Housecroft, A.G. Sharpe, Inorganic Chemistry, Prentice Hall, 2001.
[21] Ref. [20], p. 361.
[22] (a) W. Brandt, L.A. Wessjohann, ChemBioChem 6 (2005) 386;
(b) S. Gromer, L.A. Wessjohann, J. Eubel, W. Brandt, ChemBioChem 7 (2006) 1649.
[23] C.G. Zhan, D.A. Dixon, J. Phys. Chem. B 107 (2003) 4403.
[24] A. Schneider, W. Brandt, L.A. Weissjohann, Biol. Chem. 388 (2007) 1089.